Re-evaluation of bottleneck effect in coupled monolayer WS_2/photonic crystal heterostructure

Jiaru Zhou[1,2], Wenze Lan[1,2], Hao Li[1], Yu Hua[1,2], Peng Fu[1,2], Geng Li[1,2], Xiaofeng Fan[3], Changzhi Gu[1,2*], Baoli Liu[1,2*]

[1]Beijing National Laboratory for Condensed Matter Physics, Institute of Physics, Chinese Academy of Sciences, Beijing, 100190, P. R. China.
[2]School of Physical Sciences, CAS Key Laboratory of Vacuum Physics, University of Chinese Academy of Sciences, Beijing, 100190, P. R. China.
[3]College of Materials,Jilin University, No.2699 Qianjin Street, Changchun, 130012, P. R. China.

*Corresponding author(s). E-mail(s): blliu@iphy.ac.cn; czgu@iphy.ac.cn;
Contributing authors: jrzhou@iphy.ac.cn; wenzelan_96@outlook.com; hao.li@iphy.ac.cn; hua_yu@iphy.ac.cn; fupeng20@mails.ucas.ac.cn; gengli.iop@iphy.ac.cn; xffan@jlu.edu.cn;

Section S1. Extended data

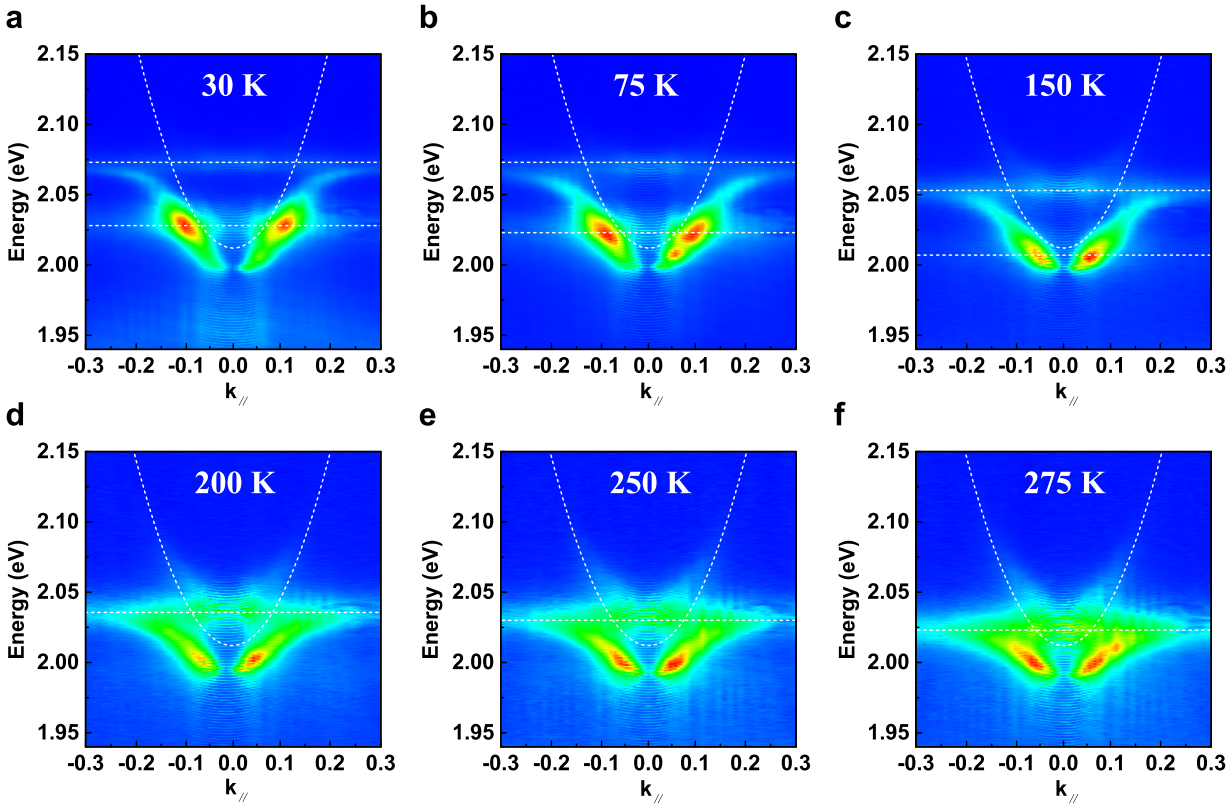

Fig. S1 Temperature-dependent evolution of momentum-resolved polariton dispersion. (a-f) Momentum-resolved PL spectra of the WS_2-PhC system measured at 30 K, 75 K, 150 K, 200 K, 250 K, and 275 K, respectively. At low temperatures (30-150 K), the position of stronger polariton emission is pinned by the trion resonance. As the temperature increases, the bottleneck behavior becomes weakened and eventually disappears at higher temperatures. This temperature-dependent evolution is consistent with the reduced thermal stability of trion at higher temperatures, which weakens their contributions to the coupling system. Consequently, the exciton-trion-photon three-mode coupling system reduces to a two-mode exciton-photon coupling system. This result provides additional support for the origin of bottleneck effect - weaker coupling strength of cavity photon-trion.

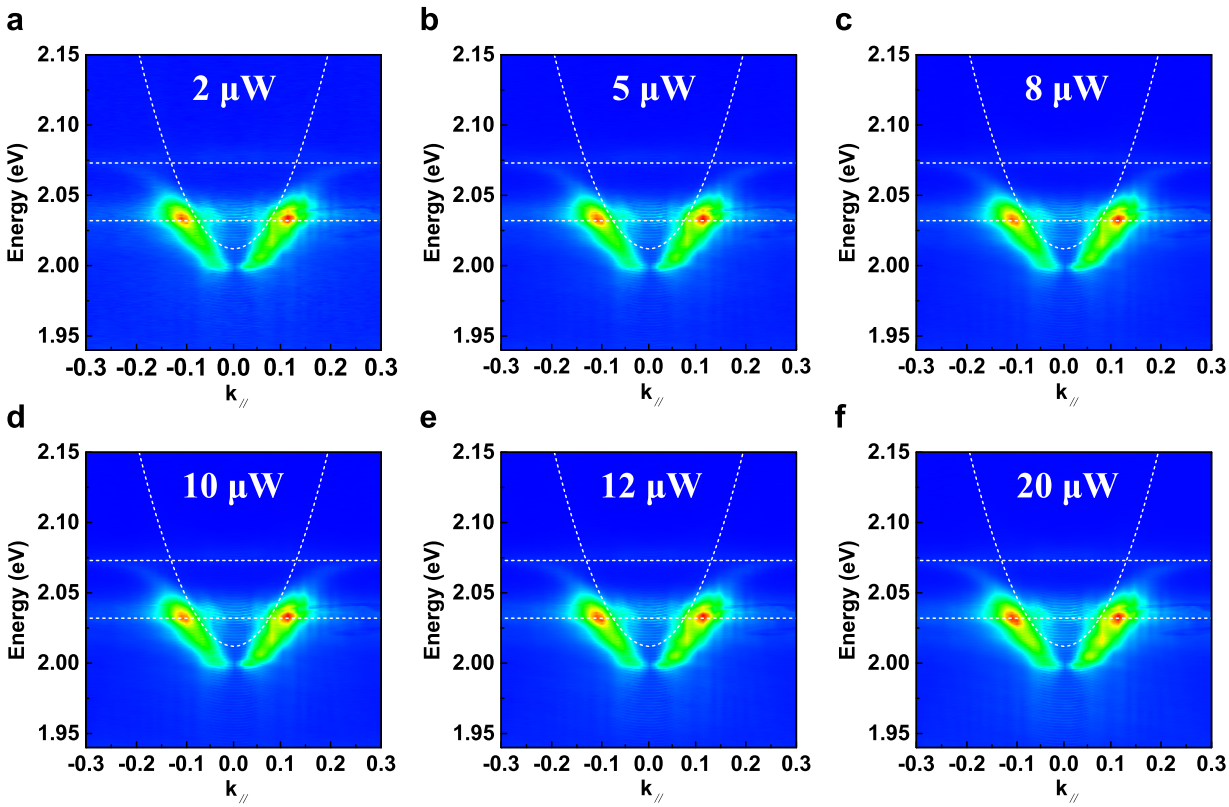

Fig. S2 Excitation-power-dependent momentum-resolved PL spectra at 12 K. Momentum-resolved PL spectra of the WS_2-PhC system measured at ∼12 K under different excitation powers: (a) 2 μW, (b) 5 μW, (c) 8 μW, (d) 10 μW, (e) 12 μW, and (f) 20 μW. Within the whole rage of the excitation powers, the polariton dispersions exhibit similar characteristics, and no pronounced bottleneck feature is observed around the anticrossing regions, which indicates that the bottleneck effect is irrelevant to the density of polaritons.

Section S2. Extraction of exciton and trion PL spectra

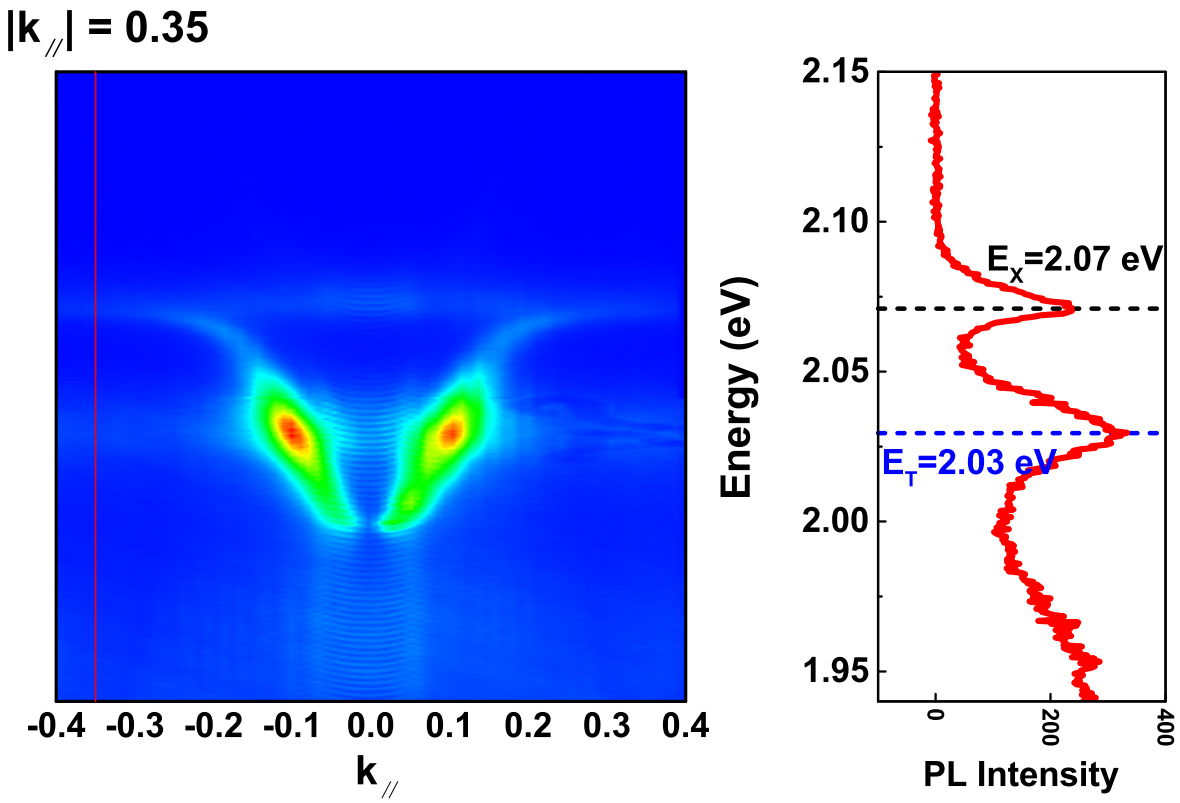

Fig. S3 Extraction method for the emission energies and line-widths of dispersionless exciton and trion. A temperature of ∼12 K is chosen as a representative example. The *Contour Profile* tool was used to extract the energy-resolved spectral linecut at the edge of the momentum-resolved PL spectra ($|k_{\|}| = 0.35$), where the coupling is weak and the emission is dominated by the uncoupled exciton and trion states. The PL spectrum extracted along the chosen momentum (or corresponding pixel point) is displayed in the right panel. Two emission peaks can be clearly identified, corresponding to the exciton at $E_{\mathrm{X}} = 2.07$ eV (black dashed line) and the trion at $E_{\mathrm{T}} = 2.03$ eV (blue dashed line), with half linewidths (half width at half maximum) of $\gamma_{\mathrm{exc}} \approx 5.5$ meV and $\gamma_{\mathrm{T}} \approx 13$ meV. Through this procedure, the energies and half linewidths of excitons and trions used in the polariton dispersion fitting are determined in the main text.

Section S3. Determination of bare PhC's photonic dispersions

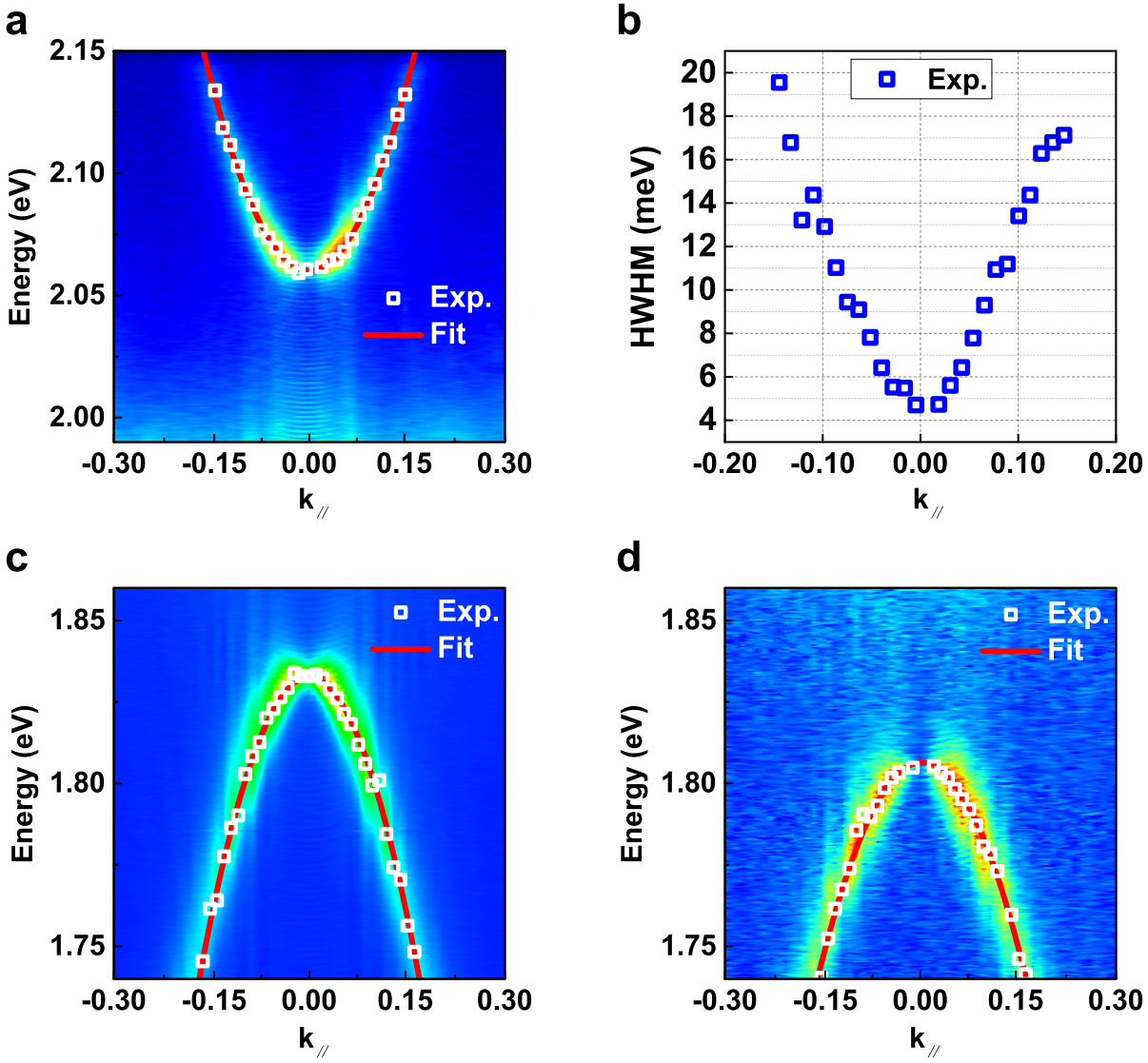

Fig. S4 Determination of the cavity-mode dispersion. Those figures illustrate the procedure used to determine the bare PhC's photonic dispersions $E_{\mathrm{cav}}(k_{\parallel}) = E_0 + ak_{\parallel}^2$ employed in the main text. (a) Momentum-resolved PL spectrum of the bare SiN_x PhC cavity before the transfer of the WS_2 monolayer. By fitting the emission peak of the cavity photon mode TE-4 shown in Fig. 1 at different in-plane momenta, a clear parabolic dispersion is obtained. In addition, the half linewidth (half-width at half-maximum) of the cavity resonance was extracted as a function of momentum as shown in (b). From this analysis, the cavity half linewidth at room temperature is estimated to be $\gamma_{\mathrm{cav}} \approx 6$ meV at $k_{\parallel} = \pm 0.04$, while at $\sim$12 K the cavity half linewidth is $\gamma_{\mathrm{cav}} \approx 13$ meV at $k_{\parallel} = \pm 0.1$. Together with the excitonic half linewidth γ_{exc}, the strong-coupling condition is satisfied. (c, d) After transferring the WS_2 monolayer onto the PhC cavity, the cavity energy exhibits an overall red-shift due to the modification of the local dielectric environment, which change the parameter E_0 in the cavity dispersion. To quantitatively estimate this red-shift, another cavity mode (TE-1 mode in Fig. 1 in the main text), which is largely detuned from the excitonic resonances and therefore does not couple with exciton and trion, is used as a reference. Panels (c) & (d) present the momentum-resolved PL spectra and corresponding fitted dispersions of the TE-1 mode before and after monolayer transfer, respectively. By comparing these spectra, a red-shift of $\sim$30 meV is obtained. This red-shift value is used to determine the energy E_0 of the TE-4 mode at Γ point after monolayer WS_2 is transferred onto the top of bare PhC with the assumption: the different cavity modes experience the same energy shift induced by the change of dielectric environment. With this red-shift value, the dispersion of the TE-4 mode is further refined through the fitting polariton dispersions, with the root-mean-square error (RMSE) smaller than $\sim$1 meV. This procedure yields the final cavity dispersion employed in the main text: $E_{\mathrm{cav}}(k_{\parallel}) = 2.012\ \mathrm{eV} + 3.47k_{\parallel}^2$.